# Visualizing inducible nitric-oxide synthase in living cells with a heme-binding fluorescent inhibitor

**Koustubh Panda*†, Mamta Chawla-Sarkar*, Cecile Santos‡, Thomas Koeck*, Serpil C. Erzurum§, John F. Parkinson¶, and Dennis J. Stuehr*†**

Departments of *Immunology and §Pathobiology, Lerner Research Institute, Cleveland Clinic, Cleveland, OH 44195; and Departments of ‡Medicinal Chemistry and ¶Immunology, Berlex Biosciences, Richmond, CA 94804

Edited by Solomon H. Snyder, Johns Hopkins University School of Medicine, Baltimore, MD, and approved May 9, 2005 (received for review December 2, 2004)

**The study of nitric-oxide synthase (NOS) physiology is constrained by the lack of suitable probes to detect NOS in living cells or animals. Here, we characterized a fluorescent inducible NOS (iNOS) inhibitor called PIF (pyrimidine imidazole FITC) and examined its utility for microscopic imaging of iNOS in living cells. PIF binding to iNOS displayed high affinity, isoform selectivity, and heme specificity, and was essentially irreversible. PIF was used to successfully image iNOS expressed in RAW264.7 cells, HEK293T cells, human A549 epithelial cells, and freshly obtained human lung epithelium. PIF was used to estimate a half-life for iNOS of 1.8 h in HEK293T cells. Our work reveals that fluorescent probes like PIF will be valuable for studying iNOS cell biology and in understanding the pathophysiology of diseases that involve dysfunctional iNOS expression.**

Nitric oxide (NO) plays a vital role in life-sustaining processes, but its overproduction has been linked to several diseases (1–5). In mammals, NO is generated through the NADPH-dependent oxidation of L-arginine (L-Arg) to NO plus citrulline catalyzed by the nitric-oxide synthases (NOSs) (6). NOS exists as three isoforms: inducible NOS (iNOS), neuronal NOS (nNOS), and endothelial NOS (eNOS) (7–9). The three NOSs display ≈50% homology in their amino acid sequences and have a similar secondary and tertiary structure (10). They are all comprised of a C-terminal flavoprotein domain that binds NADPH, FAD, and FMN, a central calmodulin-binding motif, and an N-terminal oxygenase domain that binds heme, (6*R*)-5,6,7,8-tetrahydro-L-biopterin ($H_4B$), and L-Arg (11, 12). The NOS heme is ligated to the protein through a cysteine thiolate bond (13, 14) similar to the cytochrome P450 enzymes. During NO synthesis, the NOS heme receives electrons from the flavoprotein domain and from $H_4B$ to enable a stepwise reductive activation of $O_2$ (15, 16). Besides $O_2$, the NOS heme can also bind CO, NO, CN, and imidazole as sixth ligands (17–19).

NOS must form a homodimer to become active, because this enables its flavoprotein domain to transfer electrons to the oxygenase domain where NO is made (12, 20–23). Dimer formation is part of a multistep process that creates an active NOS. The NOS polypeptide first binds FAD and FMN and then incorporates heme into the oxygenase domain. The heme-containing monomers then dimerize and bind $H_4B$ (24–26). NOS dimer formation is promoted by $H_4B$, L-Arg, and their structural analogs (21, 27–29) but can be inhibited by bulky N-substituted imidazoles like clotrimazole (29) or by the recently developed iNOS inhibitor PI (pyrimidine imidazole) (30). The selectivity and high affinity of PI toward iNOS ($K_d$ = 2.2 nM) suggests that it may be useful in down-regulating NO synthesis in diseases associated with iNOS overexpression (31). Indeed, in relevant animal models, PI was shown to prevent endotoxin-induced systemic hypotension, myocardial dysfunction, and impaired hypoxic pulmonary vasoconstriction (32), and to prevent cardiovascular and renal morbidity in a combined burn and smoke inhalation injury model (33).

The crystal structure of an iNOS monomer containing bound PI shows that its imidazole nitrogen is bound to the heme while its bulky substituents engage in steric interactions with protein structural elements that bind substrate and create the dimer interface (30). Although this structure suggests a mechanism by which PI could inhibit dimerization of iNOS monomers, it is unknown how PI interacts with iNOS in cells. We addressed this question by determining the interactions of iNOS with PI or its FITC-labeled fluorescent analog, PIF, in living cells. Our data establish the mechanism of iNOS inhibition and reveal PIF to be a valuable tool for visualizing iNOS in living cells.

## Materials and Methods

**Materials.** PI {3-[2-[(1,3-benzodioxol-5-ylmethyl) amino]-2-oxoethyl]-4-[2-(1H-imidazol-1-yl)-4-pyrimidinyl]-1-piperazinecarboxylic acid, methyl ester} and its FITC-associated analogue, PIF, were provided by Berlex Biosciences (30). The stably transfected nNOS cell line was a gift from Solomon H. Snyder and David Bredt (University of California, San Francisco). The stable eNOS expressing HEK293T cells were previously generated in our laboratory (34). Anti-iNOS monoclonal antibody was obtained from BD Transduction Laboratories, and IFN-γ was procured from Genentech. All other reagents and materials were from Sigma.

**Cloning and Expression of Fusion Protein of Human iNOS and Red Fluorescent Protein (iNOS-RFP).** Human iNOS cDNA was subcloned from an expression construct pCCF37 (35) and cloned into pDsRed-N1 (BD Clontech) with the C terminus of iNOS gene fused in-frame with the N terminus of the RFP. Expression of the iNOS-RFP in HEK293T cells was confirmed 24 h after transient transfection with Lipofectamine 2000 (Invitrogen) by immunoblot analyses and confocal immunofluorescence microscopy.

**Induction and Purification of iNOS.** Mouse macrophage RAW264.7 (RAW) cells were grown ($1 \times 10^6$ cells per ml) in 3-liter spinner culture flasks, in 10-mm-diameter tissue culture plates, or on imaging slide chambers in DMEM with 10% calf serum. The cells were induced to express iNOS with 50 μg/ml *Escherichia coli* LPS and 10 ng/ml IFN-γ as detailed in ref. 36, either in the presence or absence of 1 or 2 μM PI or PIF. Cells were harvested after 16 h of induction, washed by centrifugation at 800 rpm for 10 min in a Beckman J2-HS centrifuge and lysed by three cycles of freezing and thawing in a lysis buffer (40 mM EPPS, pH 7.6/10% glycerol/3 mM

This paper was submitted directly (Track II) to the PNAS office.

Abbreviations: $H_4B$, (6*R*)-5,6,7,8-tetrahydro-L-biopterin; NO, nitric oxide; NOS, nitric-oxide synthase; eNOS, endothelial NOS; iNOS, inducible NOS; nNOS, neuronal NOS; PI, pyrimidine imidazole; PIF, PI FITC; RAW, RAW264.7; RFP, red fluorescent protein; SA, succinyl acetone.

†To whom correspondence may be addressed at: Department of Immunology, NB3, Lerner Research Institute, Cleveland Clinic, 9500 Euclid Avenue, Cleveland, OH 44195. E-mail: pandak@ccf.org or stuehrd@ccf.org.

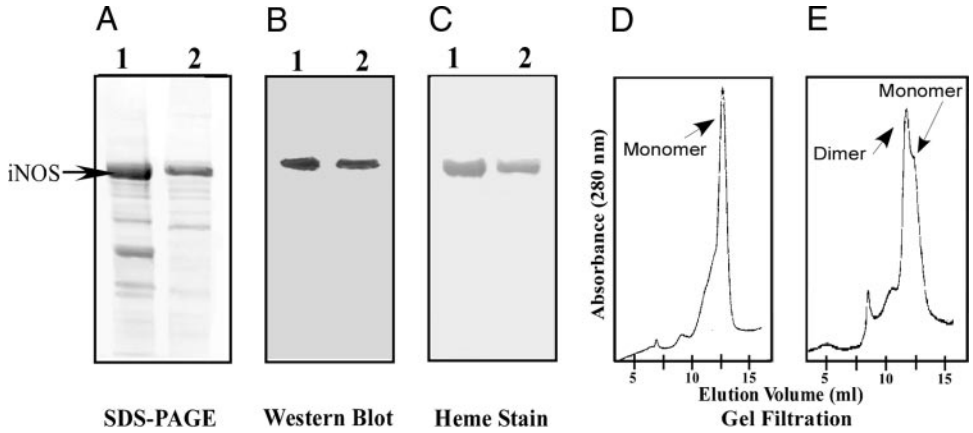


**Fig. 1.** Identification and properties of iNOS from the PI-treated RAW cells. (*A*) SDS/PAGE of the ADP-Sepharose-purified iNOS from PI-treated RAW cells (lane 1) and an authentic sample of murine iNOS standard (lane 2). (*B*) Western analysis (using an anti-iNOS antibody) of the same two samples transferred from the SDS/PAGE. (*C*) Heme staining of the same two samples. (*D* and *E*) Native gel filtration profiles of the iNOS isolated from PI-treated cells and the authentic iNOS, respectively. Results shown represent three independent experiments done under similar conditions.

DTT/100 mM NaCl/1% Nonidet P-40). The lysates were centrifuged at 20,000 rpm for 30 min in a Beckman J2-HS centrifuge and then applied to a 2′,5′-ADP (adenosine diphosphate) affinity column. The column was washed with buffer containing 40 mM EPPS, 10% glycerol, and 3 mM DTT and iNOS-eluted by using 10 mM NADPH (37). For use as controls, mouse iNOSoxy or full-length iNOS (iNOSFl) containing a $His_6$-tag were overexpressed in *E. coli* and purified (37, 38).

**Measurement of Cellular NO Synthesis.** NO production by the macrophage cells was measured at 2-h intervals by using a colorimetric assay for nitrite plus nitrate, as described in ref. 39.

**Spectral and Fluorescence Assays.** UV-visible wavelength scans were recorded at room temperature on a Hitachi U-3110 spectrophotometer. For recording the spectra of CO binding to iNOS, CO was first bubbled into the protein, dithionite was added, and the protein was scanned between 300 and 700 nm. Fluorescence was measured by using a Hitachi F-2000 spectrofluorometer.

**Confocal Microscopy.** RAW cells were induced with LPS and IFN-$\gamma$ for 16 h in the absence or presence of 0.1–2 $\mu$M PIF to determine the optimum level of the inhibitor required for visualizing the expressed iNOS in these cells. Finally, 2 $\mu$M PIF (saturation was obtained at 1 $\mu$M) was used to visualize iNOS expression in RAW cells induced by LPS and IFN-$\gamma$, A549 cells and NL-20 human lung epithelial cells induced by IFN-$\gamma$ (10 ng/ml), TNF-$\alpha$ (1 $\mu$g/ml), and IL-1$\beta$ (0.2 $\mu$g/ml), and freshly collected human bronchial epithelial (HBE) cells. Samples were collected from healthy human subjects (40) and were immediately used for experiments. The procedure was approved by the Cleveland Clinic Foundation Institutional Review Board, and written informed consent was obtained from all donors. We also used HEK293T cells transiently transfected with plasmids coding for the RFP alone (pDsRed-N1) or coding for an iNOS-RFP fusion protein to examine colocalization of iNOS with PIF. After 4 h of transfection, fresh medium was added, and the cells were grown to ≈80% confluency in four-well glass cell culture slides before being treated with PIF. In some controls, the nonfluorescent inhibitor, PI, was first added, followed by the addition of PIF, 2 h before imaging. To examine the isoform specificity of PIF in living cells, we also used HEK293T cells stably transfected with plasmids coding for eNOS and nNOS. All cells were washed three times with 1× PBS buffer and mounted in VECTASHIELD containing DAPI (Vector Laboratories). This was done after a 16-h induction period for the RAW cells, a 24-h induction period for the A549 and NL-20 cells, and 24-h after transfection for the HEK293T cells. All cells (including the HBE) were treated with PIF 2 h before mounting. Images were acquired by using a Leica TCS-SP2 laser scanning spectral confocal microscope with a ×63 oil immersion objective (numerical aperture of 1.4) at zoom 2. Laser beams of wavelengths 364, 488, and 568 nm were used to excite DAPI, FITC-labeled inhibitor, and RFP or RFP-iNOS, respectively. Emission was collected at between 400 and 500 nm for DAPI, 500 and 550 nm for FITC-labeled inhibitor, and 580 and 670 nm for RFP. Excitation and emission detection for each fluor was performed sequentially to avoid cross-talk.

**Immunocytochemical Imaging of iNOS.** RAW cells were fixed with 4% paraformaldehyde for 20 min, followed by treatment with 0.2% Triton X-100 for 5 min. They were washed twice with 1× PBS and then incubated with anti-mouse antibody (0.4 $\mu$g/ml; BD Transduction Laboratories) for 1 h, followed by Alexa Fluor 568 goat anti-mouse secondary antibody (0.5 $\mu$g/ml; Molecular Probes) for 1 h. The treated cells were then washed and subjected to confocal microscopic studies as described above.

**SDS/PAGE, Western Blot, and Heme Stain Analysis.** Gel electrophoresis of cell lysates and affinity-purified proteins was done according to the methods of Laemmli (41). After electrophoresis, the proteins were transferred to a PVDF membrane (Millipore) and Western analysis for mouse iNOS was performed. In some cases, the proteins were subjected to SDS/PAGE in the absence of 2-mercaptoethanol and then stained for heme according to standard methods (21).

**Gel Filtration Chromatography and Dimer–Monomer Content.** The affinity-purified iNOS proteins were analyzed for monomer–dimer content by gel filtration chromatography as described in ref. 42.

## Results

**The Cellular iNOS-Inhibitor Complex.** We investigated the mechanism by which PI inhibits iNOS expressed in RAW cells treated with LPS plus IFN-$\gamma$. Adding the inhibitor at 2 $\mu$M almost completely prevented NO synthesis, as evidenced through nitrite and nitrate accumulation in the culture medium, but did not affect cellular expression of heme-containing iNOS (Fig. 1*A–C*). The iNOS was predominantly monomeric in the inhibitor-

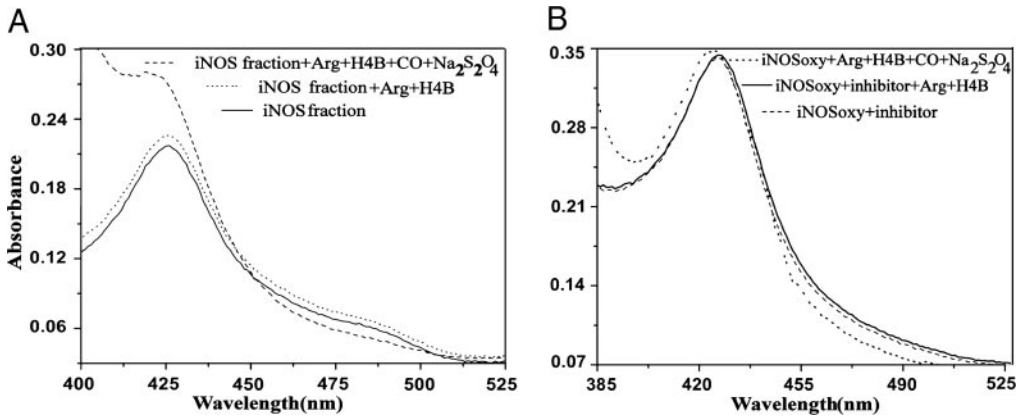


**Fig. 2.** Spectral properties of iNOS from the PI-treated RAW cells. (*A*) UV-visible spectra collected under the indicated conditions for the iNOS isolated from PI-treated RAW cells. (*B*) Spectra collected under the same conditions for a purified iNOSoxy standard that had been treated with PI. All results are representative of three independent experiments done under similar conditions.

treated cells and predominantly dimeric in the inhibitor-free cells as judged by gel-filtration chromatography (Fig. 1 *D* and *E*). When the iNOS monomer was isolated from the inhibitor-treated cells by using 2′,5′-ADP affinity chromatography and subject to spectral analysis, the spectrum showed that the enzyme contained inhibitor bound to its ferric heme as judged by a Soret absorbance at 427 nm (Fig. 2*A*), which is characteristic of an imidazole-bound heme-thiolate protein (29). Remarkably, the stability of the iNOS ferric heme-inhibitor complex was such that it was unable to undergo dithionite-mediated heme reduction and CO binding (Fig. 2*A*). The properties of the iNOS that we isolated from the PI-treated cells were confirmed in experiments done with purified iNOSoxy (Fig. 2*B*). Together, the results suggest a mechanism whereby the inhibitor binds to heme-containing iNOS monomers as they appear within the activated cells. Formation of the iNOS heme-inhibitor complex is essentially irreversible, consistent with an extremely slow $k_{off}$ value estimated for the enzyme–inhibitor complex (31). This leads to a cellular accumulation of heme-containing iNOS monomers that cannot associate into active dimeric iNOS because of the tightly bound inhibitor.

**Fluorescent Inhibitor Binding to iNOS.** We next examined iNOS interaction with the fluorescent FITC-tagged inhibitor analog (PIF). Adding PIF to purified iNOS that was free of $H_4B$ and L-Arg caused a shift in the heme Soret absorbance peak from 414 to 427 nm (Fig. 3*A*), indicating that PIF binds to iNOS in the same manner as the PI; namely, through ligation of its imidazole nitrogen to the ferric heme iron. There was a partial quenching of PIF fluorescence when it bound to iNOS (Fig. 3*B*), consistent with its binding to the heme.

**Fluorescent Imaging of iNOS in Cells.** Our above results suggested that PIF could visualize iNOS in living cells. We used fluorescence confocal microscopy to explore this possibility in RAW cells induced by LPS and IFN-γ, in A549 cells and human NL-20 lung epithelial cells induced by IFN-γ, TNF-α, and IL-1β, and in freshly collected HBE cells. We also used HEK293T cells that were transfected to transiently express human iNOS, which in some cases was tagged at its C terminus with RFP (iNOS-RFP) for examining the specificity of PIF interaction with iNOS. All cells were prestained with a nucleus staining dye (DAPI) to help demarcate the location of the iNOS protein within the cells. Fig. 4 *A* and *B* shows fluorescent images of macrophage RAW cells that had been given PIF along with LPS and IFN-γ to induce iNOS expression. A punctate green fluorescence is apparent in the cytosol of the washed, living cells after 16 h of induction. The fluorescence was not observed in cells that received PIF without LPS and IFN-γ (Fig. 4*C*). Thus, the appearance of the punctate green fluorescence correlated with iNOS expression. Similarly, adding PIF enabled visualization of human iNOS expressed in the cytokine-induced A549 or NL-20 lung epithelial cell lines (Fig. 4 *D* and *E*) and in freshly collected HBE cells (Fig. 4*F*). We next added PIF to HEK293T cells that were transiently expressing the human iNOS-RFP. Fig. 4 *G–I* shows the same cell field as scanned for iNOS-RFP expression, for the green fluorescent

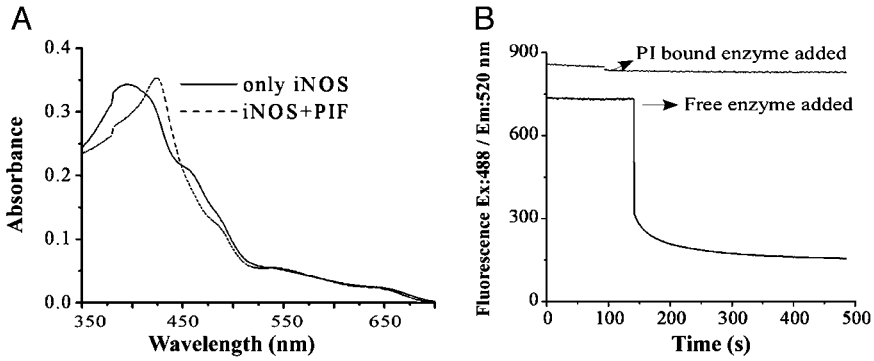


**Fig. 3.** Visible and fluorescent changes upon PIF binding to iNOS. (*A*) Light absorbance spectra of purified iNOS before and after PIF addition. (*B*) Change in PIF (0.1 μM) fluorescence intensity upon addition of an excess iNOS protein sample (2 μM) that either contained bound PI or was free from it. Data are representative of three independent experiments done under similar conditions.

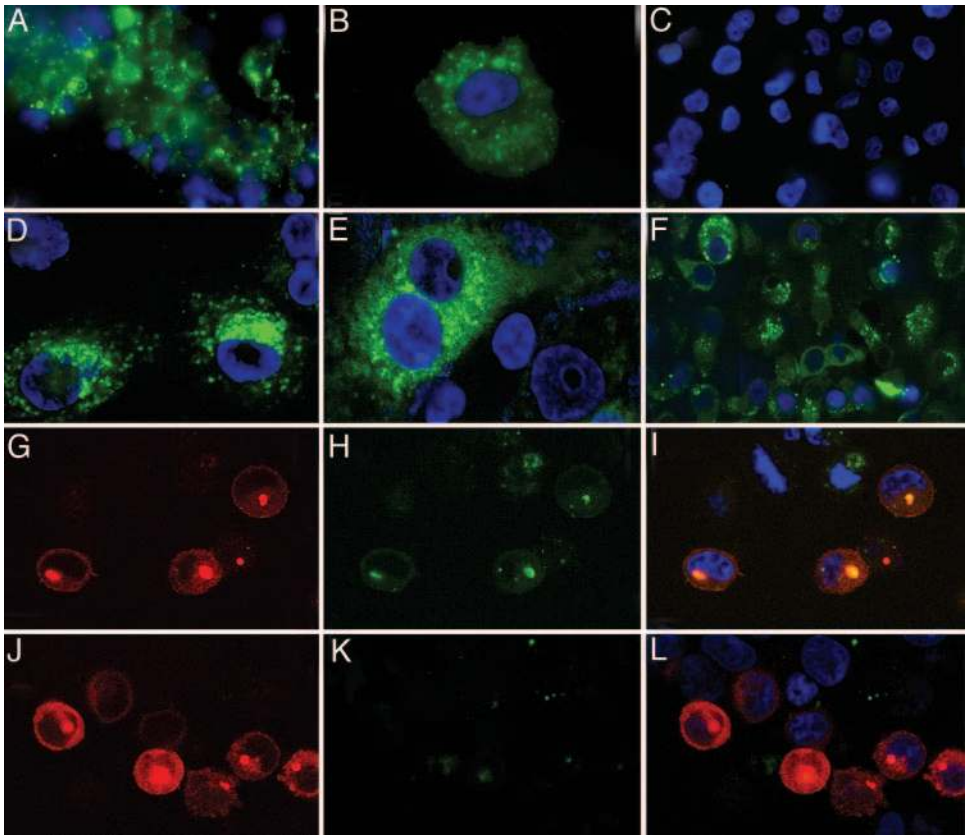


**Fig. 4.** Fluorescent and confocal imaging of the PIF–iNOS interaction in living cells. Various cells expressing iNOS were cultured with 2 $\mu$M PIF, washed, and subjected to fluorescent imaging microscopy. Green, PIF; blue, nucleus-staining dye, DAPI; red, iNOS-RFP protein. (*A*) RAW cells were induced for iNOS expression with LPS (50 $\mu$g/ml) and IFN-$\gamma$ (10 ng/ml). (*B*) A $\times$40 image of a single cell from *A*. (*C*) PIF-treated, noninduced RAW cells. (*D* and *E*) PIF-treated human A549 and NL-20 cells that were induced for iNOS expression with IFN-$\gamma$ (10 ng/ml), TNF-$\alpha$ (1 $\mu$g/ml), and IL-1$\beta$ (0.2 $\mu$g/ml), respectively. (*F*) Freshly collected HBE cells after PIF treatment for 2 h. (*G–I*) HEK293T cells transfected with human-iNOS-RFP. (*G*) Red fluorescence of iNOS-RFP. (*H*) Green fluorescence of bound PIF. (*I*) Overlay of *G* and *H*. (*J–L*) HEK293T cells transfected with pDsRed-N1 alone, in the same presentation sequence as described for *G–I*. Lipofectamine-transfected cells undergoing apoptosis showed nonspecific green autofluorescence at 488 nm excitation as seen in the background of *H*, *I*, *K*, and *L*. Data shown are representative of three independent experiments done under similar conditions.

iNOS inhibitor, and a confocal overlay of these two scans, respectively. The yellow-orange spots in Fig. 4*I* indicate the colocalization of iNOS-RFP and the green PIF in these cells. We did not observe a colocalization of red and green fluorescence when HEK293T cells that were expressing RFP alone were treated with PIF (Fig. 4 *J–L*) or when cells expressing the iNOS-RFP had been pretreated for 8 h with the nonfluorescent inhibitor PI before the addition of PIF (data not shown). These data demonstrate specific PIF-iNOS binding in a range of cell types that are expressing iNOS naturally or in response to transfection.

We next examined whether PIF binding correlates with inhibition of iNOS activity in cells. Fig. 5 shows that PIF binding to iNOS in induced RAW cell cultures was only observed when the PIF concentration was sufficient to inhibit cellular NO synthesis. This result further demonstrates the specificity of PIF binding. We then determined the half-life of PIF-bound iNOS monomer in HEK293T cells that were transiently transfected with human iNOS and then treated with PIF and cyclohexamide (to stop further iNOS expression). Fig. 7, which is published as supporting information on the PNAS web site, summarizes the results and indicates that the half-life of the PIF-bound human iNOS monomer was 1.8 h in HEK293T cells. This value agrees with the half-life of iNOS as determined by other means (43).

We also examined the NOS isoform specificity of PIF binding. Fig. 6 *A*, *C*, and *E* shows nNOS-, eNOS-, and iNOS-expressing cells after treatment with 1 $\mu$M PIF for 2 h. PIF binding was observed only in cells expressing iNOS, although NOS protein expression was apparent in all cases from the respective immunostains (Fig. 6 *B*, *D*, and *F*). Treatment of cells with SA, a heme biosynthesis inhibitor, has been observed to produce heme-free NOS (25). We therefore treated RAW cells with 250 $\mu$M SA for 48 h to deplete heme stores before inducing the cells with LPS and IFN-$\gamma$. Fig. 6 shows that PIF binding in the SA-treated cells (*G*) was insignificant compared with its binding in induced cells that did not receive SA (*E*), despite similar iNOS protein expression (*F* and *H*). An iNOS heme-CO binding assay (P450 assay) was performed on the cell lysates to confirm that iNOS from the SA-treated cells was largely in a heme-free form (Fig. 6*I*). These experiments established that PIF binding is iNOS-specific and requires bound heme.

## Discussion

**Mechanism of PIF Interaction with iNOS.** Our previous studies with N1-substituted imidazole inhibitors of iNOS showed that they all bind to the heme in a purified iNOS monomer and form stable heme-inhibitor complexes that resist dimerization promoted by $H_4B$ and L-Arg (29). When clotrimazole (an inhibitor of this class) was added to cells expressing iNOS, it prevented iNOS dimerization and NO synthesis and resulted in an accumulation of iNOS monomers that were, in fact, heme-free (29). This finding implied that clotrimazole blocked iNOS dimerization in

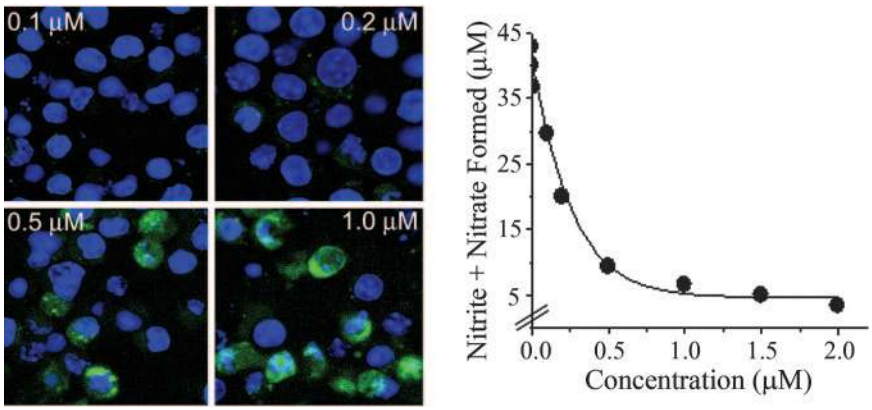


**Fig. 5.** Correlation between PIF binding and inhibition of iNOS NO synthesis activity in cells. (*Left*) RAW cells induced to express iNOS by treatment with LPS (50 $\mu$g/ml) and IFN-$\gamma$ (10 ng/ml) for 16 h in the presence of the indicated concentrations of PIF. (*Right*) Nitrite plus nitrate production over 16 h by the activated RAW cell cultures as a function of PIF concentration. Data are representative of three separate experiments done under similar conditions.

cells by preventing heme incorporation into NOS. However, in our current study the iNOS monomers we isolated from PI-treated cells were in the form of a iNOS heme–PI complex, suggesting distinct mechanisms of inhibition for PI versus clotrimazole. PI binds to heme-containing iNOS monomers in the cells and thus prevents their dimerization. This mechanism is supported by the crystal structure of the iNOS monomer–PI complex, which shows that portions of the PI molecule sterically interact with protein elements that help form the iNOS dimer interface (30).

**Advantages of PIF Imaging of iNOS.** PIF presents an effective way to visualize and target iNOS in living cells. Established immunocytochemical/histochemical (ICH) methods are generally unsuitable for use in living cells or tissues, which must be fixed and made permeable with cytocidal detergent before antibody staining. Such methods suffer from inherent constraints of epitope cross-reaction and nonspecific background interference. To visualize iNOS with PIF, one needs to simply incubate cells for 30–40 min, wash, mount, and observe with a fluorescent microscope. The short preparation time can be critical when iNOS expression is transiently stable or stops after cell harvesting. One such example is iNOS expression in HBE cells, which is important in diseases like asthma and bronchitis (44). These cells showed substantial iNOS expression when freshly collected and stained with PIF in our study, whereas when the same cells are immunostained, almost no iNOS is observed. This outcome is apparently because the comparatively longer ICH procedure risks the loss of a large part of the endogenous iNOS (44). Indeed, the use of PIF obviates the need for multiple wash steps and does not require that the cells be fixed or mounted, which are typical in ICH methods and often lead to loss of weakly adherent cells. Some groups have also expressed NOS-GFP constructs to visualize NOS and study its movement in living cells (45–47). However, this method is limited to cells that are transfected with a NOS-GFP fusion gene and thus cannot address the more typical circumstances of cells expressing NOS naturally or after transfection with a NOS DNA. PIF can visualize iNOS in all of these settings. The specificity, affinity, and irreversibility of PIF binding to iNOS suggest that it could be used to sort and quantify iNOS-containing cells from mixed populations, to track expression and movement of iNOS under the microscope, and to differentiate heme-containing and heme-free forms of iNOS in cells. Moreover, it may likely enable visualization of iNOS in the whole animal, particularly in disease models that involve its dysfunction. Thus, PIF may help advance our understanding of iNOS cell biology in a broad spectrum of physiological and pathological settings.

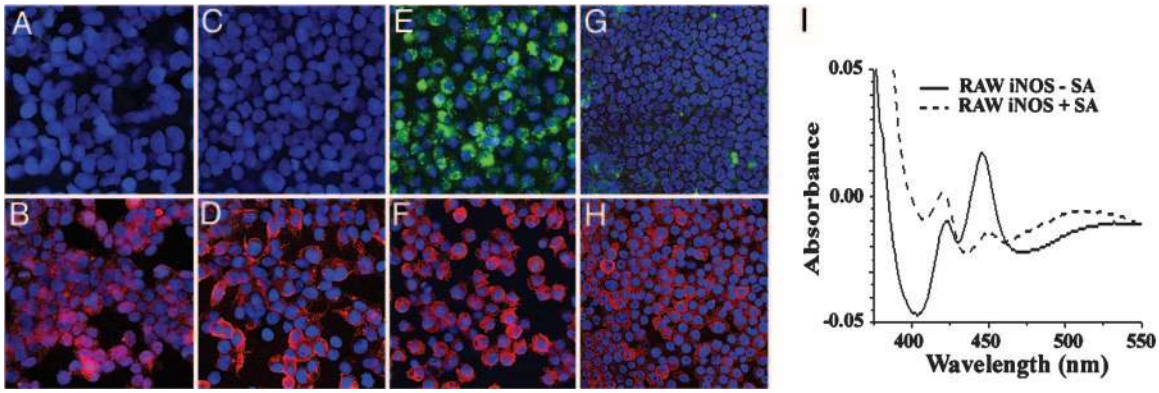


**Fig. 6.** Isoform and heme specificity of PIF. HEK293T cells stably transfected with plasmids expressing nNOS (*A*) and eNOS (*C*) were treated with 1 $\mu$M PIF for 2 h along with RAW cells induced to express iNOS (*E*). RAW cells were also pretreated with 250 $\mu$M succinyl acetone (SA) for 48 h to block heme biosynthesis and thereafter treated with LPS (50 $\mu$g/ml) and IFN-$\gamma$ (10 ng/ml) to induce iNOS expression and then treated with 1 $\mu$M PIF for 2 h (*G*) as the SA-untreated RAW cells (*E*). A companion set of all of the PIF-treated cells (*A*, *C*, *E*, and *G*) were immunostained with respective NOS immunofluorescent antibodies after fixing (*B*, *D*, *F*, and *H*). (*I*) Aliquots of cell lysate from both SA-treated and untreated cells containing equivalent protein were reduced with dithionite, given CO, and scanned in a spectrophotometer. The peak at 444 nm indicates the concentration of iNOS heme in each cell lysate. Data shown are representative of three independent experiments done under similar conditions.

We thank Dr. Amit Vasanji of the Cleveland Clinic Foundation Imaging Core for his expert support. This work was supported, in part, by National Institutes of Health Grants GM51491 (to D.J.S.), CA53919 (to D.J.S.), HL076491 (to D.J.S.), and AI70649 (to S.C.E.).

1. Harrison, D. G. (1997) *J. Clin. Invest.* **100,** 2153–2157.
2. MacMicking, J., Xie, Q. W. & Nathan, C. (1997) *Annu. Rev. Immunol.* **15,** 323–350.
3. Gross, S. S. & Wolin, M. S. (1995) *Annu. Rev. Physiol.* **57,** 737–769.
4. Michel, T. & Feron, O. (1997) *J. Clin. Invest.* **100,** 2146–2152.
5. Schmidt, H. H. W. & Walter, U. (1994) *Cell* **78,** 919–925.
6. Griffith, O. W. & Stuehr, D. J. (1995) *Annu. Rev. Physiol.* **57,** 707–736.
7. Marletta, M. A. (1994) *Cell* **78,** 927–930.
8. Forstermann, U., Gath, I., Schwarz, P., Closs, E. I. & Kleinert, H. (1995) *Biochem. Pharmacol.* **50,** 1321–1332.
9. Wang, Y., Goligorsky, M. S., Lin, M., Wilcox, J. N. & Marsden, P. A. (1997) *J. Biol. Chem.* **272,** 11392–11401.
10. Dinerman, J. L., Lowestein, C. J. & Snyder, S. H. (1993) *Circ. Res.* **73,** 217–222.
11. Hemmens, B. & Mayer, B. (1998) *Methods Mol. Biol.* **100,** 1–32.
12. Stuehr, D. J. (1999) *Biochim. Biophys. Acta* **1411,** 217–230.
13. Sono, M., Stuehr, D. J., Ikeda-Saito, M. & Dawson, J. H. (1995) *J. Biol. Chem.* **270,** 19943–19948.
14. McMillan, K., Bredt, D. S., Hirsch, D. J., Snyder, S. H., Clark, J. E. & Masters, B. S. S. (1992) *Proc. Natl. Acad. Sci. USA* **89,** 11141–11145.
15. Wei, C. C., Crane, B. R. & Stuehr, D. J. (2003) *Chem. Rev.* **103,** 2365–2383.
16. Gorren, A. C. & Mayer, B. (2002) *Curr. Drug Metab.* **3,** 133–157.
17. Pufahl, R. A. & Marletta, M. A. (1993) *Biochem. Biophys. Res. Commun.* **193,** 963–970.
18. Wolff, D. J., Datto, G. A., Samatovicz, R. A. & Tempsick, R. A. (1993) *J. Biol. Chem.* **268,** 9425–9429.
19. Abu-Soud, H. M., Wang, J., Rousseau, D. L., Ignarro, L. J. & Stuehr, D. J. (1995) *J. Biol. Chem.* **270,** 22997–23006.
20. Baek, K. J., Thiel, B. A., Lucas, S. & Stuehr, D. J. (1993) *J. Biol. Chem.* **268,** 21120–21129.
21. Klatt, P., Pfeiffer, S., List, B. M., Lehner, D., Glatter, O., Bachinger, H. P., Werner, E. R., Schmidt, K. & Mayer, B. (1996) *J. Biol. Chem.* **271,** 7336–7342.
22. Rodriguez-Crespo, I., Gerber, N. C. & Ortiz de Montellano, P. R. (1996) *J. Biol. Chem.* **271,** 11462–11467.
23. Panda, K., Ghosh, S. & Stuehr, D. J. (2001) *J. Biol. Chem.* **276,** 23349–23356.
24. Stuehr, D. J. (1997) *Annu. Rev. Pharmacol. Toxicol.* **37,** 339–359.
25. Albakri, Q. A. & Stuehr, D. J. (1996) *J. Biol. Chem.* **271,** 5414–5421.
26. Hemmens, B., Gorren, A. C., Schmidt, K., Werner, E. R. & Mayer, B. (1998) *Biochem. J.* **332,** 337–342.
27. Sennequier, N. & Stuehr, D. J. (1996) *Biochemistry* **35,** 5883–5892.
28. Presta, A., Siddhanta, U., Wu, C., Sennequier, N., Huang, L., Abu-Soud, H. M., Erzurum, S. C. & Stuehr, D. J. (1998) *Biochemistry* **37,** 298–310.
29. Sennequier, N., Wolan, D. & Stuehr, D. J. (1999) *J. Biol. Chem.* **274,** 930–938.
30. McMillan, K., Adler, M., Auld, D. S., Baldwin, J. J., Blasko, E., Browne, L. J., Chelsky, D., Davey, D., Dolle, R. E., Eagen, K. A., *et al.* (2000) *Proc. Natl. Acad. Sci. USA* **97,** 1506–1511.
31. Blasko, E., Glaser, C. B., Devlin, J. J., Xia, W., Feldman, R. I., Polokoff, M. A., Phillips, G. B., Whitlow, M., Auld, D. S., McMillan, K., *et. al.* (2002) *J. Biol. Chem.* **277,** 295–302.
32. Ichinose, F., Hataishi, R., Wu, J. C., Kawai, N., Rodrigues, A. C., Mallari, C., Post, J. M., Parkinson, J. F., Picard, M. H., Bloch, K. D. & Zapol, W. M. (2003) *Am. J. Physiol.* **285,** H2524–H2530.
33. Enkhbaatar, P., Murakami, K., Shimoda, K., Mizutani, A., Traber, L., Phillips, G., Parkinson, J., Salsbury J. R., Biondo, N., Schmalstieg, F., *et al.* (2003) *Am. J. Physiol.* **285,** H2430–H2436.
34. Presta, A., Liu, J., Sessa, W. C. & Stuehr, D. J. (1997) *Nitric Oxide* **1,** 74–87.
35. Xu, W., Kaneko, F. T., Zheng, S., Comhair, S. A., Janocha, A. J., Goggans, T., Thunnissen, F. B., Farver, C., Hazen, S. L., Jennings, C., *et al.* (2004) *FASEB J.* **18,** 1746–1748.
36. Stuehr, D. J. & Marletta, M. A. (1987) *Cancer Res.* **47,** 5590–5594.
37. Siddhanta, U., Wu, C., Abu-Soud, H. M., Zhang, J., Ghosh, D. K. & Stuehr, D. J. (1996) *J. Biol. Chem.* **271,** 7309–7312.
38. Wu, C., Zhang, J., Abu-Soud, H. M, Ghosh, D. K. & Stuehr, D. J. (1996) *Biochem. Biophys. Res. Commun.* **222,** 439–444.
39. Miranda, K. M., Espey, M. G. & Wink, D. A. (2001) *Nitric Oxide* **5,** 62–71.
40. De Raeve, H. R., Thunnissen, F. B., Kaneko, F. T., Guo, F. H., Lewis, M., Kavuru, M. S., Secic, M., Thomassen, M. J. & Erzurum, S. C. (1997) *Am. J. Physiol.* **272,** L148–L154.
41. Laemmli, U. K. (1970) *Nature* **227,** 680–685.
42. Panda, K., Rosenfeld, R. J., Ghosh, S., Meade, A. L., Getzoff, E. D. & Stuehr, D. J. (2002) *J. Biol. Chem.* **277,** 31020–31030.
43. Kolodziejski, P. J., Koo, J. S. & Eissa, N. T. (2004) *Proc. Natl. Acad. Sci. USA* **101,** 18141–18146.
44. Guo, F. H., Comhair, S. A., Zheng, S., Dweik, R. A., Eissa, N. T., Thomassen, M. J., Calhoun, W. & Erzurum, S. C. (2000) *J. Immunol.* **164,** 5970–5980.
45. van Haperen, R., Cheng, C., Mees, B. M., van Deel, E., de Waard, M., van Damme, L. C., van Gent, T., van Aken, T., Duncker, D. J. & de Crom, R. (2003) *Am. J. Pathol.* **163,** 1677–1686.
46. Yoshitake, J., Akaike, T., Akuta, T., Tamura, F., Ogura, T., Esumi, H. & Maeda, H. (2004) *J. Virol.* **78,** 8709–8719.
47. Ji, J. Y. & Diamond, S. L. (2004). *Biochem. Biophys. Res. Commun.* **318,** 192–197.